Published in final edited form as:
BJU Int. 2009 March ; 103(6): 826–835. doi:10.1111/j.1464-410X.2008.08195.x.

Face-specific binding of prothrombin fragment 1 and human serum albumin to inorganic and urinary calcium oxalate monohydrate crystals

Alison F. Cook, **Phulwinder K. Grover**, and **Rosemary L. Ryall**
Department of Surgery, Flinders University School of Medicine, Flinders Medical Centre, Bedford Park, South Australia, Australia

Abstract

Objective—To compare the intracrystalline distributions of prothrombin fragment 1 (PTF1) and human serum albumin (HSA) within inorganic and urinary calcium oxalate (CaOx) monohydrate (COM) crystals and to determine whether binding of PTF1 can be explained by interactions between particular γ-carboxyglutamic (Gla) residues and atomic arrays on individual faces of the COM crystal.

Materials and methods—COM crystals were precipitated from inorganic solutions and ultrafiltered urine containing fluorescent HSA or PTF1 at different relative concentrations and examined by fluorescence microscopy. Accelrys Materials Studio and Discovery Studio were used to model the binding of PTF1 to the top, side and apical faces of the COM crystal.

Results—PTF1 alone always adsorbed predominantly to the COM apical surfaces, while HSA bound principally to the side faces under inorganic conditions, but to the apical faces in urine. In the presence of each other, both proteins competed for adsorption to the apical faces, with attachment of PTF1 dominating over that of HSA. Modelling showed that urinary PTF1 had equal theoretical bonding potential for all three COM surfaces.

Conclusions—(i) Anisotropic inclusion of HSA and PTF1 into urinary and inorganic COM crystals results from their preferential binding to specific COM faces; (ii) the binding preference of HSA differs under inorganic and urinary conditions; (iii) preferential binding of PTF1 to the apical faces of COM is more complex than can be explained by interactions between Gla groups and surface atomic arrays; (iv) future studies of interactions between urinary proteins and stone mineral crystal surfaces should be performed in urine.

Keywords

calcium oxalate; urolithiasis; intracrystalline protein; prothrombin fragment 1; human serum albumin; biomineralization

Introduction

The construction of healthy biominerals involves several well recognized, though poorly understood steps, one of which is interfacial or molecular recognition [1]. This phenomenon is directed by genetically determined domains in proteins [2], which are electrostatically,

Correspondence: Professor Rosemary Lyons Ryall, Department of Surgery, Flinders Medical Centre, Bedford Park, South Australia 5042, Australia. rose.ryall@flinders.edu.au.

Conflict of Interest
None declared.

geometrically and stereochemically complementary to specific sites on the crystal lattice [1]. Epitaxial alignment of the protein molecule with the crystal surface at their interface guarantees the nucleation of a mineral with a defined composition, shape, size, texture and orientation, and with the requisite physical properties to fulfil the specific functions required by living organisms. In many instances the proteins become incarcerated within the biomineral during its formation [3,4].

Human kidney stones are biologically induced biominerals [5] composed principally of calcium oxalate (CaOx) which, like their salubrious counterparts, always contain a macromolecular matrix distributed throughout the entire structure. Until recently, only 20 or so stone matrix proteins had been identified immunologically or by amino acid sequence analysis [6]. Although > 68 have now been identified in the matrix of CaOx monohydrate (COM) stones [7], it is most unlikely that they all fulfil specific roles in stone formation. Urine contains hundreds of proteins derived from glomerular filtration, active cellular secretion, routine tissue turnover and epithelial injury inflicted by the stone itself. To identify proteins actively involved in stone formation while excluding those produced by stone-related cellular injury, studies have focused on proteins irreversibly associated with CaOx crystals generated from fresh human urine [8,9]. Relatively few of the many proteins present in healthy urine have been unambiguously identified in the soluble organic extract remaining after demineralization of COM crystals precipitated from human urine [9], included among which are human serum albumin (HSA) and a urinary form of prothrombin fragment 1 (PTF1) [9–11]. Despite its presence in stone and the COM crystal matrix, HSA has little effect on CaOx crystallization and consequently has not featured prominently in the stone literature [12]. On the other hand, PTF1 is synthesized in the human kidney [13], is present in calcium stones [14], and potently inhibits CaOx crystal growth and crystal aggregation [15–17]. The inhibitory properties of the molecule are undoubtedly conferred by a domain located near its N-terminus, which contains 10 residues of γ-carboxyglutamic acid (Gla), through which it binds to the CaOx crystal surface [16,17]. Figure 1. shows the common structure of urinary COM (uCOM) and inorganic COM (iCOM) crystals [18–26].

Irrespective of whether biominerals are classified as matrix-mediated or biologically induced [5], the binding of proteins to their crystal building blocks must rely on compatibility between the physical configuration of the protein and the atomic array on the crystal face. At present, relatively little is known about the means by which urinary protein molecules align with and attach to the CaOx crystal surface and become incorporated into the final crystal bulk. Recently, studies have begun to examine the interactions between some urinary constituents, particularly citrate and osteopontin, and COM crystal surfaces, but the existence of numerous crystallographic forms of COM and the use of at least seven different unit cell choices [27] have made direct comparison of published findings difficult. Figure 1 shows the common structure of COM crystals usually seen in human urine (A, B and D) or grown from inorganic solutions (C), showing the Miller indexes assigned to the dominant faces by recent authors. Wesson [18–20] and Hunter [24,25] and their colleagues use the notation system of Tazzoli and Domeneghetti [26], while Qiu and coworkers [21–23] use that of Deganello and Piro [28]. To avoid confusion and to facilitate comparison of published findings, in this paper the three dominant faces of COM are referred to as top, side and apical (Fig. 1D).

One method for observing selective attachment of a molecule to a particular crystal face is to grow the crystal in its presence after labelling it with a fluorescent tag, which can produce distribution patterns known as intersectoral zoning (Fig. 2). The formation of ‘bow-tie’ patterns in crystals occurs when a protein labelled with a fluorescent or coloured dye adsorbs strongly to one particular face, but interacts only weakly with the others. As growth and adsorption proceed, bow-tie patterns will develop. Such patterns have been observed for

many years in ‘dye-inclusion crystals’ in which the intracrystalline distribution of colour reflects the preferential attachment of the dye to individual crystal faces [29]. Our aim in the present study was to determine whether HSA and PTF1 attach preferentially to any of the three dominant faces of COM by labelling them with fluorescent tags and observing their distribution within COM crystals generated from inorganic solutions and from ultrafiltered urine to which they had been added. PTF1 was found to bind preferentially to the apical surfaces of both iCOM and uCOM crystals. To assess whether this specificity could be related to atomic motifs on the crystal surface, we used the Accelrys program to model possible contacts between the Gla groups of the PTF1 molecule and calcium atoms on the top, side and apical faces of the COM crystal.

Materials and methods

HSA (catalogue number A8763–5G) was purchased from Sigma-Aldrich (MO, USA) and used without further purification. Human PTF1, which was purified and characterized by SDS-PAGE and Western blotting as described previously [30], migrated as a single band at 31 kDa. All other chemicals were of the highest analytical quality available.

PTF1 and HSA were labelled with fluorescein isothiocyanate (FITC) using a ProtOn Fluorescein Labeling kit (Vector Laboratories, CA, USA). A separate HSA sample was labelled with Alexa Fluor 647 dye using an Alexa Fluor 647 Protein Labeling kit (Molecular Probes, Inc., OR, USA).

With the approval of the Flinders Clinical Research Ethics Committee, urine samples were collected from healthy donors, with their informed consent, and shown to be free of blood and nitrites by dipstick analysis (Combur^7 Test®, Roche Diagnostics). The urines were pooled and treated with 0.02% sodium azide, and the pooled sample was centrifuged at 20 °C and 10–000 ***g*** for 30 min (J2–21 M/E, Beckman Instruments, Fullerton, CA, USA). The urine was then filtered through a 0.22-μm filter (GVWP14250, Millipore Corporation, Billerica, MA, USA), and the calcium concentration determined by the o-cresophthalein complexone technique, using an automated biochemical analyser, at a wavelength of 546 nm. The calcium concentration was brought to 2 mmol/L by the addition of filtered (0.22 μm) $CaCl_2$ solution and the pH was adjusted to 6.1 using concentrated HCl. A portion of the sample was then ultrafiltered using a PrepScale TFF cartridge (Millipore Corporation, Bedford, MA, USA) with a molecular weight threshold of 10 kDa.

Preparation of COM crystals

In inorganic solutions, additives affect crystallization at concentrations 1/10th to 1/100th of those required in undiluted urine [31]. The mean normal urinary concentration of PTF1 is ≈13.4 nmol/L [32] which, given a molecular mass of ≈30 kDa, converts to≈0.42 mg/L. HSA occurs in urine at concentrations up to ≈20 mg/L [33], or ≈300 nmol/L for a molecular mass of ≈65 kDa. Thus, different concentrations of PTF1 and HSA were used in the preparation of the iCOM and uCOM crystals. When necessary, protein concentrations were also adjusted to ensure that sufficient fluorescence was obtained to observe intersectoral zoning.

To prepare iCOM crystals, 7.5 mL of $CaCl_2$ (5 mmol/L) containing different concentrations of FITC-labelled protein(s), was added to separate conical flasks, which were placed in a shaking water bath at 37 °C. 7.5 mL of 5 mM sodium oxalate (NaOx) solution was added dropwise using a syringe pump (Razel, model A-99) over a 2.5-h period and the flasks were then refrigerated at 4 °C for ≈ 48 h. The final protein concentrations were: *PTF1 dose–response experiment*: 0, 0.01, 0.05 and 0.5 mg/L of PTF1 (FITC-labelled); *HSA alone*: 5 mg/L (FITC-labelled); *PTF1 + HSA at equal concentrations*: 0.05 mg/L PTF1 (FITC-labelled),

0.05 mg/L HSA (Alexa-647-labelled); *PTF1 + HSA at approximate urinary concentration ratio*: 0.04 mg/L PTF1 (FITC-labelled) and 2.0 mg/L HSA (Alexa-647-labelled).

For uCOM crystals, crystals were generated from ultrafiltered urine using the same procedure as above, except that the NaOx solution was 7 mM and ultrafiltered urine was used in place of $CaCl_2$ solution. Final protein concentrations were: *PTF1 dose–response experiment*: 0, 0.25, 0.5, 1 and 2 mg/L of PTF1 (FITC-labelled); *HSA alone*: 20 mg/L (FITC-labelled); *PTF1 + HSA at approximate urinary concentration ratio*: 1 mg/L PTF1 (FITC-labelled) and 20 mg/L HSA (Alexa-647-labelled).

Controls consisted of iCOM and uCOM crystals generated in the absence of proteins. Additional controls comprised iCOM and uCOM crystals grown without proteins, but in the presence of either FITC or Alexa Fluor 647, at dye concentrations equivalent to the amount of dye calculated to bind at the highest protein concentrations. All crystals were washed five times with distilled water to remove excess superficial protein.

For fluorescence microscopy, crystals were examined using an Olympus AX70 fluorescence microscope equipped with a Hamamatsu digital camera fitted with appropriate filters for the FITC and Alexa-647 dyes, the excitation and emission maxima of which are sufficiently different that each can be examined separately in the same sample without interference from the other.

Computer modelling

Atomic coordinates for COM [26] were entered into the Accelrys Materials Studio program (San Diego, CA 92121, USA: Version 4.0) to produce three-dimensional (3D) images of the top, side and apical faces of COM. Using the Accelrys Discovery Studio program the structure of bovine PTF1 (Protein Data Bank: file number 2PF2) was used to display the F1 file from the Protein Data Bank as a ribbon diagram showing the Gla groups and their associated bound calcium atoms. This was imported into Materials Studio and rotated manually so that its Gla domain was facing the top, side or apical surface of the COM crystal.

Human PTF1 lacks a residue corresponding to glycine at position 4 in the bovine molecule, as a result of which numbering of the Gla residues differs by 1 (Table 1). Bovine PTF1 binds seven calcium atoms, while the human F1 molecule binds an eighth, which Li *et al*. [34] assigned to Gla 32. X-ray crystallographic information is not available for human PTF1, but using the available bovine data [35], Li *et al*. [34] derived the corresponding human structure and showed that the 3D configurations of the two molecules were remarkably similar, as were coordinations between their common seven calcium ions and Gla groups. We therefore assumed that modelled contacts between Gla groups of the bovine molecule and the COM crystal surface would apply equally to human PTF1.

Gla groups 15, 20, 21, 26, 30 and 33 are located on the exterior of the PTF1 structure and could therefore potentially bond with a surface, but the molecule's 3D shape precludes their contact with the same flat surface at any one time. Only Gla residues 15 and 20, or 20 and 21, or 26, 30 and 33 would be able to contact the COM surface simultaneously; that is, the highest number of Gla's that could together bond with a flat COM surface is three. Thus, the modelling focused on bonding between COM and Gla residues 26, 30 and 33. Gla groups 26 and 30 together bind Ca-1 [34], which was removed for the purposes of the model. Possible interactions between Gla residues 26, 30 and 33 and each of the three COM faces were constructed by manoeuvring the PTF1 molecule into the best potential bonding arrangement that could be achieved by eye. As the sum of the atomic radii of oxygen and calcium is ≈2.43–2.46 Å [36], modelling assumed a distance of at least 2.45 Å between the carboxylate

oxygen atoms of the Gla's and the surface calcium atoms. Using Accelrys, the distances between the Gla oxygen atoms and COM surface calcium atoms were measured, and if the distance between them was > 2.45 Å but less than the arbitrary distance of 6 Å, the measurement was accepted as a possible bonding arrangement. The possibility of repulsive forces between the negatively charged Gla groups and the oxalate molecules on the COM crystal surfaces was not taken into account.

Bonding via direct interaction between calcium atoms coordinated to the Gla groups of PTF1 and oxalate molecules on the COM surfaces was also modelled. Of the seven calcium atoms bound to bovine PTF1, Ca-2, Ca-3, Ca-4 and Ca-5 are buried within the Gla domain [34,35], leaving Ca-1, Ca-6 and Ca-7 potentially available for bonding with COM. The eighth calcium atom in human PTF1 was coordinated to Gla 32 [34]. Thus four calcium atoms are potentially available in the human molecule for complexation with oxalate on the COM surface. However, only Ca-6 (coordinated to Gla 19 and Gla 20) and Ca-7 (coordinated to Gla 14 and Gla 19) [34] could contact a flat surface simultaneously, as indicated by modelling studies of bovine PTF1 [37], which show Ca-6 and Ca-7 in close proximity protruding above the electrostatic potential surface of the molecule's Gla domain. Therefore possible interactions of Ca-6 and Ca-7 with oxalates on the top, side and apical surfaces of COM were constructed using Accelrys in a similar manner to that described above.

Results

Pure iCOM crystals did not autofluoresce, and in the absence of added protein, uCOM crystals displayed only a very weak autofluorescence distributed evenly throughout the crystals. Both iCOM and uCOM crystals grown in the presence of the Alexa-647 dye displayed no fluorescence under either filter, other than the weak autofluorescence just mentioned.

Incorporation of PTF1 into iCOM and uCOM crystals

Intracrystalline fluorescence patterns of FITC-labelled iCOM and uCOM crystals precipitated in the presence of increasing concentrations of PTF1 are shown in Fig. 3. With no added PTF1, significant fluorescence was absent from the iCOM crystals and very slight fluorescence was seen in the uCOM crystals. Only weak fluorescence was visible in the iCOM crystals at PTF1 concentrations of 0.01 and 0.05 mg/L, distributed very faintly around the periphery and in the crystal centre. At 0.50 mg/L, fluorescence was distributed predominantly in a bow-tie pattern consistent with preferential binding to the apical faces.

The fact that it did not extend to the crystal boundaries indicates that crystal growth continued after solution supplies of the protein had been exhausted. Faint fluorescence, which may have resulted from minor adsorption to the top face, was visible throughout the crystal. This pattern was repeated in the uCOM crystals, which showed fluorescence consistent with little or no binding to the side faces, some limited adsorption to the top faces, and strong binding to the apical faces, which increased proportionally with protein concentration. The protein was also concentrated at the crystal centres, particularly at 1 and 2 mg/L.

Comparison of PTF1 and HSA incorporation into iCOM and uCOM crystals

The intracrystalline distributions of PTF1 and HSA are compared in Fig. 4. As before, under both inorganic and urinary conditions, PTF1 was incorporated anisotropically in a bow-tie pattern consistent with minor adsorption to the top crystal face and stronger binding to the apical faces. In contrast, HSA adsorbed principally to the side faces of the iCOM crystals, as

shown by the strongly fluorescing bow-tie orientated across the short axis of the crystal (top right panel, Fig. 4). It also bound to the apical faces, though less strongly. Thus, under inorganic conditions HSA binds preferentially to the side faces of the COM crystal, but will also bind to the apical faces. However, the fluorescence distribution in the uCOM crystals (Fig. 4) showed that for most of the growth period HSA bound principally to the apical faces, though still with some binding to the side faces, suggesting that other urinary components can interfere with the attachment of HSA to the side surfaces.

Incorporation of PTF1 and HSA in mixtures of both proteins

Crystals generated in inorganic solutions containing both proteins at the same concentration (0.05 mg/L) are shown in row A of Fig. 5.

As was seen when the proteins were tested separately, weak fluorescence was visible throughout the crystals, suggesting minor binding to the top crystal faces. PTF1 was again distributed mainly in a bow-tie pattern indicative of adsorption to the apical surfaces, while that of HSA was consistent with preferential adsorption to the side faces. The different anisotropic incorporation of each protein into the crystal was also evident when the two separate patterns were overlaid, as shown in the right panel in row A of Fig. 5. When both proteins were present at a likely urinary concentration ratio (PTF1–0.04 mg/L, HSA 2.0 mg/L), PTF1 fluorescence was consistent with binding principally to the apical faces and some attachment to the top faces (Fig. 5, row B) early during crystal growth. However, HSA now fluoresced strongly throughout the centre of the crystal in a pattern suggesting attachment to both the apical *and* side faces. As discussed above, in an aqueous solution containing an equivalent concentration of PTF1, HSA attached principally to the side faces. However, when present at a much higher concentration than PTF1, HSA was able to compete more successfully for binding sites on the apical surfaces. This likelihood is supported by the fluorescence patterns in uCOM crystals precipitated from ultrafiltered urine containing both PTF1 and HSA at concentrations of 2 mg/L and 20 mg/L, respectively (row C, Fig. 5). PTF1 again bound preferentially to the COM apical faces, but the distribution of fluorescent HSA was restricted largely to two narrow bands indicating adsorption to the apical faces late in the crystal's formation: as shown in Fig. 3, there was little binding to the side faces.

As proposed above, in ultrafiltered urine HSA is probably prevented from binding to the side faces by one or more unidentified urinary components with superior binding affinity for those surfaces. It is also apparent that the concentration of PTF1 (2 mg/L or ≈ 65 nM) was sufficient to exclude HSA from binding sites on the apical faces in the early stages of the crystal's growth, despite HSA's presence at five-fold the molar concentration (20 mg/L or ≈300 nM). Once the less abundant PTF1 had been depleted from solution and fresh mineral had been deposited, additional binding sites would have then become available on the apical faces, allowing the more plentiful HSA to adsorb. This supposition is supported by the fact that the points where the intense fluorescence from PTF1 ends correspond with the positions at which intense fluorescence from HSA begins (Fig. 5).

Modelling of PTF1 adsorption to the top, side and apical faces of the COM crystal

Modelled interactions of carboxylate oxygen atoms of Gla residues 26, 30 and 33 with calcium atoms on the top, side and apical faces of COM are shown in Fig. 6. Nine Gla oxygen atoms can bond with surface calcium atoms on all three COM faces, and these involve the same number of interactions with each of the Gla carboxylate oxygen atoms: all four oxygens on Gla 26, two on Gla 30, and three on Gla 33. Thus, the three COM surfaces have the same potential for bonding to PTF1. Because this finding seemed at odds with the results of the fluorescence study, simulations of possible interactions between PTF1's

complexed calcium ions and oxygens of the oxalate groups on each crystal surface were also performed.

As was found with the interactions between the Gla carboxylates and COM surface calcium atoms, the three COM crystal faces have the same potential to bind to PTF1, as Ca-6 and Ca-7 can potentially coordinate with eight oxygen atoms of the oxalate groups on all of them (Fig. 7). Side perspective views of the molecular structure of the three COM surfaces were therefore constructed to identify any features of the crystalline lattice structure that might explain PTF1's binding selectivity.

As is well described [20,21], two types of oxalate ions occur in the COM crystal lattice, one of which is parallel to the surface plane while the other is perpendicular. As shown in Fig. 8, the perpendicular oxalates on the top crystal face lie beneath the outermost crystal surface, in which calcium and parallel oxalate ions lie in the same plane.

On the apical face the perpendicular oxalates are angled, so that only one of the four oxygen atoms of each oxalate lies on the surface layer, together with adjacent calcium ions. However, on the side face the perpendicular oxalate groups protrude above the layer containing coplanar water molecules, lattice calcium ions and parallel oxalate ions.

Discussion

The possibility that proteins might be buried inside individual stone crystals was first raised when it was shown that the demineralized extracts of uric acid [38] and CaOx [8] crystals precipitated from urine contained relatively few of the proteins present in the urine itself. Studies of the organic matrix of CaOx crystals precipitated from fresh, healthy human urine were extended by Doyle *et al*. [9] who confirmed that protein inclusion is selective and reported the predominance of a 30-kDa protein (now known to be PTF1), and emphasized that the proteins had originated from within the mineral bulk. The presence of organic material within ghosts of demineralized CaOx crystals from human stones [39] and crystalluric particles experimentally induced in rats [39,40] was later shown by transmission electron microscopy, while biochemical analysis [41], field emission electron microscopy [42,43] and synchrotron X-ray diffraction [44] were used to confirm the intracrystalline location of proteins in crystals precipitated from healthy urine.

Using a similar approach to that adopted by Touryan *et al*. [45], who studied the incorporation of protein G into COM, the present study showed that PTF1 was incorporated anisotropically and in a dose-dependent manner into both uCOM and iCOM crystals in a bow-tie pattern consistent with some binding to the top crystal surfaces, but principally to the apical faces. In keeping with a previous report [43], the present study also showed that fluorescence was focused at the crystal core, particularly in uCOM crystals. PTF1 is therefore associated with mineral from the point of nucleation and may induce precipitation by the process of templating. HSA, on the other hand, clearly binds to the side faces of the iCOM crystal, although it also shows some adsorption to the apical surfaces, indicating that in the absence of competing molecules it prefers to attach to the side faces of COM. However, if all available binding sites on the side faces are occupied (in this instance probably because of its own high concentration), HSA will bind by default to the apical faces, as shown by the reversal of the fluorescence bow-tie pattern in COM precipitated from ultrafiltered urine, in which it bound to the side faces. The ultrafiltered urine used would have contained low molecular weight species such as citrate, pyrophosphate and magnesium, which are well known to affect COM crystallization, as well as numerous organic compounds, and proteins and peptides with molecular masses of < 10 kDa. Other than citrate, which binds specifically to the top faces of COM [21,22], one or more of those

molecules apparently competed successfully for binding sites on the side COM surfaces and prevented HSA from attaching. The identity of the urinary competitor(s) is unknown, but it must have a stronger affinity for the COM crystal surface than HSA and been present at a sufficiently high concentration throughout crystal growth to force a high proportion of the HSA molecules to attach to the apical faces.

When iCOM crystals were generated from inorganic solutions containing both PTF1 and HSA at the same concentration, their intracrystalline distributions were identical to those seen when each protein was incorporated separately, with PTF1 binding predominantly to the apical faces and HSA to the side faces. At an approximate physiological concentration ratio of the two proteins, the distribution of PTF1 was unaltered. In contrast, HSA exhibited fluorescence consistent with equal affinity for both the side and apical faces, probably because its higher molar concentration allowed it to compete successfully for binding sites on the apical crystal faces. This likelihood is strengthened by the distribution patterns seen when COM crystals were precipitated from ultrafiltered urine containing PTF1 and HSA at approximate urinary concentrations. PTF1 again bound principally to the apical faces. However, HSA did not bind to the side faces, fluorescence being restricted to a narrow band at each end of the crystal. This arrangement suggested, as discussed above, that HSA was prevented from binding to the side faces by other low molecular mass urinary components, but also to the apical faces, by PTF1. Because the molar concentration of PTF1 was much lower than that of HSA, it would have been more rapidly exhausted from solution, leaving binding sites on the apical faces available for attachment of the more abundant HSA and resulting in the crescent-shaped fluorescent band at each end of the crystal.

Thus, the attachment of urinary HSA and PTF1 to growing COM crystals is face-specific and competitive, and both proteins are interred within single crystals. Previous work examining the interaction of urinary proteins with individual faces of COM has been scarce. Sheng *et al*. [20] measured adhesion forces between coated atomic-force microscope tips and COM crystals immersed in solutions of various proteins and showed that HSA bound with equal affinity to the top, side and apical faces of COM, and osteopontin bound preferentially to the top face. Using a different atomic-force microscopy approach, Qiu *et al*. [21] reported that osteopontin bound to the side faces of growing COM crystals and strongly retarded solute deposition by step-specific pinning, though having little effect on the top faces to which it bound relatively weakly. They attributed the divergent effects on the two faces to differences in geometrical compatibilities between functional domains in the osteopontin molecule and crystal steps and terraces, as well as disparities in step heights between the two faces. More recently, Taller *et al*. [24] used scanning confocal microscopy combined with fluorescence imaging to show that osteopontin adsorbs with high specificity to the edges between the top and apical faces of iCOM crystals and much less to any of the faces themselves. Given the disparities between their observations and those described previously [20,21], it is clear that interactions are determined by step height and structure, in addition to molecular matching between functional groups on the osteopontin molecule and the arrangement of lattice ions on each crystal surface.

The requirement of the Gla domain for human PTF1 and prothrombin to inhibit CaOx crystallization [16,17] relies on the fact that of all the amino acids, Gla adsorbs most strongly to crystalline COM [46]. However, not all of the 10 Gla residues in the Gla domain are available for binding, some being submerged within the PTF1 folded structure. Modelling was therefore based first on the premise that binding of the PTF1 molecule to the COM crystal surface is mediated by interaction between the carboxylate ions of Gla groups 26, 30 and 33 and COM surface calcium ions. This showed that all faces had the same potential for bonding to PTF1, which was unexpected, in view of the results of the fluorescent studies. We therefore considered the possibility that the attachment of PTF1 to

COM could occur via direct interaction between Ca-6 and Ca-7 of the protein and negatively charged oxygen ions of surface oxalate molecules. Since, again, there were no obvious reasons for the binding preferences of PTF1, atomic models of the faces were constructed.

As is well known and has been recently re-emphasized [19,20], the atomic arrangements of calcium and oxalate ions differ markedly between the top, side and apical faces of COM crystals, as is shown in Fig. 8. If binding of PTF1 to COM were occurring via interactions between oxalate ions and calcium atoms coordinated to PTF1, projection of the carboxylate groups above the topmost layer would seem to favour binding of the protein to the side faces. However, the fluorescence study showed that PTF1 actually bound very little to those surfaces. On the other hand, the lack of binding to the side faces can be explained if attachment of the protein were mediated by binding between calcium ions on the top and apical faces and Gla residues 26, 30 and 33, whose carboxylates are easily accessible. Because the Ca^{2+} surface densities of the top, apical and side faces decrease in the order 0.054 $Ca^{2+}/Å^2$ > 0.041 $Ca^{2+}/Å^2$ > 0.033 $Ca^{2+}/Å$ [19], PTF1 would be likely to adsorb more to the top surface and less to the apical face. Binding to the top face would also be encouraged by the flat orientation of oxalate groups on its surface, as it would avoid electrostatic repulsion of the Gla carboxylates by electronegative ends of oxalate molecules. On the other hand, projection of the carboxylate moieties of the perpendicular oxalate groups beyond the topmost layer of the side face would repel the carboxylates in the Gla residues and prevent attachment of PTF1, as has been offered as an explanation for citrate's preferred binding to the top face of COM [21–23]. This would also explain why PTF1 binds to the top and apical COM faces and does not adhere to the side faces, particularly as the Gla domain is very electronegative [35], and can account for the strong binding of PTF1 to the apical faces and weak adsorption to the top faces. Nonetheless, the observed bow-tie pattern would still have resulted even if PTF1 had bound equally to both the top and apical faces. As shown in Fig. 2, binding to the top face would produce fluorescence throughout the crystal and attachment to the apical faces would produce a bow-tie pattern along its length. The combined effect would be a bow-tie pattern at each end of the crystal resulting from fluorescence contributed by both the top and apical faces, while in the side regions there would be fluorescence only from PTF1 bound to the side faces. Although this interpretation concurs with the weak fluorescence seen throughout most of the crystal, together with the brighter fluorescence at both ends (Figs 4 and 5), the relative lack of fluorescence seen along the crystal sides, particularly those of the urinary crystals in Figs 4 and 5, certainly indicates that PTF1 binds more avidly to the apical faces than to the top surfaces. However, modelling was unable to explain this selectivity, possibly because adsorption is the net result of numerous factors:

- The magnitude of the energy required for an adsorbent to bind to a COM crystal surface depends upon calcium spacing, step-riser angle and height, hydroxyl to oxalate distance and electrostatic interactions [47], not all of which were taken into account in the present model.
- The nonplanar geometry of growth steps provides the most favourable environment for the attachment of citrate to the COM crystal surface [22]. If PTF1 also binds in the region of advancing steps, interactions between its structural elements and crystal lattice ions would occur simultaneously on terraces and adjacent step risers, which the present modelling did not accommodate.
- The calcium-stabilized crystallized conformation of crystallized PTF1 upon which the modelling was based may be different in solution.
- Attachment of PTF1 to the phospholipid membrane during blood clotting involves amino acid residues other than Gla [34], as well as multiple influences including ionic, van der Waals and hydrophobic forces [37]. It is probable therefore, that

binding of PTF1 to COM is also determined, at least partly, by additional forces and other amino acid residues in the Gla domain, which were not considered in the present model.

- Binding of PTF1 to the phospholipid membrane during blood coagulation appears to occur via bridges formed with calcium ions in the environment [48]. Thus in urine, where calcium levels can be as high as 8–10 mmol/L, solution calcium ions could act as bridges to mediate binding between structures on the PTF1 molecule and the COM crystal surface.

Factors such as these, all of which would be impossible to accommodate, undoubtedly limit the physiological applicability of purely theoretical models. For instance, Gul and Rez [49] modelled the adsorption of seven different proteins to the COM top face on the basis of possible interactions between crystal surface calcium ions and protein carboxylate groups in aspartic acid, glutamic acid or Gla residues. Because all the proteins were able to contact the crystal surface simultaneously at only three or four contact points, they concluded that their interactions with COM are weak, which seems contrary to the observation that at least two of the proteins they examined, PTF1 [9–11] and bikunin [50], bind so strongly to the growing COM crystal surface that they are included into the mineral bulk.

Knowing the distribution of proteins within COM can produce useful information about their molecular interactions with crystal surfaces, which, in combination with other techniques such as atomic force microscopy and computer modelling may assist in identifying factors that dictate binding preference and thus provide a rational basis for medical stone therapy. However, it is clear that protein adsorption is subject to influences far more complex than the number of contact points or simple interactions between functional groups in proteins and inorganic crystal surface lattice ions under aqueous conditions. The development of pharmacological agents for stone prevention should therefore include investigations that use urinary crystals and are performed in human urine.

Acknowledgments

We gratefully acknowledge Grant No. NDDK 1 R01 DK064050–01A1 from the National Institutes of Health, USA. Alison Cook was the recipient of a Flinders University Postgraduate Scholarship.

Abbreviations

(i)(u)COM	(inorganic) (urinary) CaOx monohydrate
HSA	human serum albumin
PTF1	prothrombin fragment 1
Gla	γ-carboxyglutamic acid
FITC	fluorescein isothiocyanate
3D	three-dimensional

References

1. Mann S. Molecular tectonics in biomineralization and biomimetic materials chemistry. Nature. 1993; 365:499–505.
2. Heuer AH, Fink DJ, Laraia VJ, et al. Innovative materials processing strategies: a biomimetic approach. Science. 1992; 255:1098–105. [PubMed: 1546311]
3. Berman A, Addadi L, Weiner S. Interactions of sea-urchin skeleton macromolecules with growing calcite crystals – a study of intracrystalline proteins. Nature. 1988; 331:546–8.

4. Aizenberg J, Ilan M, Weiner S, Addadi L. Intracrystalline macromolecules are involved in the morphogenesis of calcitic sponge spicules. Connect Tissue Res. 1996; 34:255–61. [PubMed: 9084634]
5. Veis A. Mineralization in organic matrix frameworks. Rev in Miner Geochem. 2003; 54:249–89.
6. Ryall, RL.; Cook, AF.; Thurgood, LA.; Grover, PK. In: Evans, AP.; Lingeman, JE.; Williams, JC., Jr , editors. Macromolecules relevant to stone formation; Renal stone disease: 1st annual international urolithiasis research symposium: Indianapolis; Indiana. 2–3 November 2006; Melville, NY: American Institute of Physics; 2007. p. 129-40.
7. Canales BK, Anderson L, Higgins L, et al. Second prize: comprehensive proteomic analysis of human calcium oxalate monohydrate kidney stone matrix. J Endourol. 2008; 22:1161–7. [PubMed: 18484873]
8. Morse RM, Resnick MI. A new approach to the study of urinary macromolecules as participant in calcium oxalate crystallization. J Urol. 1988; 139:869–73. [PubMed: 3352063]
9. Doyle IR, Ryall RL, Marshall VR. Inclusion of proteins into calcium oxalate crystals precipitated from human urine: a highly selective phenomenon. Clin Chem. 1991; 37:1589–94. [PubMed: 1893595]
10. Stapleton AM, Ryall RL. Crystal matrix protein – getting blood out of a stone. Miner Electrolyte Metab. 1994; 20:399–409. [PubMed: 7783703]
11. Ryall RL, Grover PK, Thurgood LA, Chauvet MC, Fleming DE, van Bronswijk W. The importance of a clean face: the effect of different washing procedures on the association of Tamm-Horsfall glycoprotein and other urinary proteins with calcium oxalate crystals. Urol Res. 2007; 35:1–14. [PubMed: 17277922]
12. Ryall, RL. Macromolecules and kidney stone formation: Waste of space or space for waste?. In: Segura, J.; Khoury, S.; Pak, C.; Preminger, GM.; Tolley, D., editors. Stone Disease. Paris: Health Publications Editions; 2003. p. 69-79.
13. Stapleton AM, Timme TL, Ryall RL. Gene expression of prothrombin in the human kidney and its potential relevance to kidney stone disease. Br J Urol. 1998; 81:666–72. [PubMed: 9634038]
14. Stapleton AM, Dawson CJ, Grover PK, et al. Further evidence linking urolithiasis and blood coagulation: urinary prothrombin fragment 1 is present in stone matrix. Kidney Int. 1996; 49:880–8. [PubMed: 8648933]
15. Ryall RL, Grover PK, Stapleton AMF, et al. The urinary F1 activation peptide of human prothrombin is a potent inhibitor of calcium oxalate crystallization in undiluted human urine *in vitro*. Clin Sci (Lond). 1995; 89:533–41. [PubMed: 8549069]
16. Grover PK, Ryall RL. Inhibition of calcium oxalate crystal growth and aggregation by prothrombin and its fragments *in vitro*: relationship between protein structure and inhibitory activity. Eur J Biochem. 1999; 263:50–6. [PubMed: 10429186]
17. Grover PK, Ryall RL. Effect of prothrombin and its activation fragments on calcium oxalate crystal growth and aggregation in undiluted human urine in vitro: relationship between protein structure and inhibitory activity. Clin Sci (Lond). 2002; 102:425–34. [PubMed: 11914105]
18. Guo S, Ward MD, Wesson JA. Direct visualization of calcium oxalate monohydrate crystallization and dissolution with atomic force microscopy and the role of polymeric additives. Langmuir. 2002; 18:4284–91.
19. Jung T, Sheng X, Choi CK, Kim WS, Wesson JA, Ward MD. Probing crystallization of calcium oxalate monohydrate and the role of macromolecule additives with *in situ* atomic force microscopy. Langmuir. 2004; 20:8587–96. [PubMed: 15379479]
20. Sheng X, Jung T, Wesson JA, Ward MD. Adhesion at calcium oxalate crystal surfaces and the effect of urinary constituents. Proc Natl Acad Sci USA. 2005; 102:267–72. [PubMed: 15625112]
21. Qiu SR, Wierzbicki A, Orme CA, et al. Molecular modulation of calcium oxalate crystallization by osteopontin and citrate. Proc Natl Acad Sci USA. 2004; 101:1811–5. [PubMed: 14766970]
22. Qiu SR, Wierzbicki A, Salter A, et al. Modulation of calcium oxalate monohydrate crystallization by citrate through selective binding to atomic steps. J Am Chem Soc. 2005; 127:9036–44. [PubMed: 15969581]
23. De Yoreo JJ, Qiu SR, Hoyer JR. Molecular modulation of calcium oxalate crystallization. Am J Physiol Renal Physiol. 2006; 291:F1123–32. [PubMed: 17082348]

24. Taller A, Grohe B, Rogers KA, Goldberg HA, Hunter GK. Specific adsorption of osteopontin and synthetic polypeptides to calcium oxalate monohydrate crystals. Biophys J. 2007; 93:1768–77. [PubMed: 17496021]
25. Grohe B, O'Young JO, Ionescu A, et al. Control of calcium oxalate crystal growth by face-specific adsorption of an osteopontin phosphopeptide. J Am Chem Soc. 2007; 129:14946–51. [PubMed: 17994739]
26. Tazzoli V, Domeneghetti C. The crystal structures of whewellite and weddellite: re-examination and comparison. Am Miner. 1980; 65:327–34.
27. Millan A. Crystal growth shape of whewellite polymorphs: influence of structure distortions on crystal shape. Cryst Growth Des. 2001; 1:245–54.
28. Deganello S, Piro OE. The crystal structure of calcium oxalate monohydrate (whewellite). Neues Jahrb Mineral. 1981; 2:81–8.
29. Kahr B, Gurney RW. Dyeing crystals. Chem Rev. 2001; 101:893–951. [PubMed: 11709861]
30. Grover PK, Moritz RL, Simpson RJ, Ryall RL. Inhibition of growth and aggregation of calcium oxalate crystals *in vitro* – a comparison of four human proteins. Eur J Biochem. 1998; 253:637–44. [PubMed: 9654060]
31. Hess B, Ryall RL, Kavanagh JP, et al. Methods for measuring crystallization in urolithiasis research. why, how and when? Eur Urol. 2001; 40:220–30. [PubMed: 11528202]
32. Bezeaud A, Guillin MC. Quantitation of prothrombin activation products in human urine. Br J Haematol. 1984; 58:597–606. [PubMed: 6549141]
33. Roberts, WL.; McMillin, GA.; Burtis, CA., et al. Reference Information for the Clinical Laboratory. In: Burtis, CA.; Ashwood, ER.; Bruns, DE., editors. Teitz Textbook of Clinical Chemistry and Molecular Diagnostics. 4. Vol. Chapt 56. St Louis: Elsevier Saunders; 2006. p. 2254Section VII
34. Li L, Darden T, Foley C, Hiskey R, Pedersen L. Homology modeling and molecular dynamics simulation of human prothrombin fragment 1. Protein Sci. 1995; 4:2341–8. [PubMed: 8563631]
35. Søriano-Garcia M, Padmanabhan K, de Vos AM, Tulinsky A. The Ca^{2+} ion and membrane binding structure of the Gla domain of Ca-prothrombin fragment 1. Biochemistry. 1992; 31:2554–66. [PubMed: 1547238]
36. Megyes T, Bakó I, Bálint S, Grósz T, Radnai T. Ion pairing in aqueous calcium chloride solution: molecular dynamics simulation and diffraction studies. J Mol Liquids. 2006; 129:63–74.
37. Huang M, Rigby AC, Morelli X, et al. Structural basis of membrane binding by Gla domains of vitamin K-dependent proteins. Nat Struct Biol. 2003; 10:751–6. [PubMed: 12923575]
38. Iwata H, Kamei O, Abe Y, et al. The organic matrix of urinary uric acid crystals. J Urol. 1988; 139:607–10. [PubMed: 3343752]
39. Khan SR. Calcium phosphate/calcium oxalate crystal association in urinary stones: implications for heterogeneous nucleation of calcium oxalate. J Urol. 1997; 157:376–83. [PubMed: 8976301]
40. Boevé ER, Ketelaars GAM, Vermeij M, Cao LC, Schröder FH, De Bruijn WC. An ultrastructural study of experimentally induced microliths in rat proximal and distal tubules. J Urol. 1993; 149:893–9. [PubMed: 8455270]
41. Ryall RL, Chauvet MC, Grover PK. Intracrystalline proteins and urolithiasis: a comparison of the protein content and ultrastructure of urinary calcium oxalate monohydrate and dihydrate crystals. BJU Int. 2005; 96:654–63. [PubMed: 16104927]
42. Ryall RL, Fleming DE, Grover PK, Chauvet MC, Dean CJ, Marshall VR. The hole truth: intracrystalline proteins and calcium oxalate kidney stones. Mol Urol. 2000; 4:391–402. [PubMed: 11156707]
43. Ryall RL, Fleming DE, Doyle IR, Evan NA, Dean CJ, Marshall VR. Intracrystalline proteins and the hidden ultrastructure of calcium oxalate urinary crystals: Implications for kidney stone formation. J Struct Biol. 2001; 134:5–14. [PubMed: 11469872]
44. Fleming DE, van Reissen A, Chauvet MC, et al. Intracrystalline proteins and urolithiasis: a synchrotron X-ray diffraction study of calcium oxalate monohydrate. J Bone Miner Res. 2003; 18:1282–91. [PubMed: 12854839]
45. Touryan LA, Clark RH, Gurney RW, Stayton PS. Incorporation of fluorescent molecules and proteins into calcium oxalate monohydrate single crystals. J Cryst Growth. 2001; 233:380–8.

46. Fleming DE, van Bronswijk W, Ryall RL. A comparative study of the adsorption of amino acids on calcium minerals found in renal calculi. Clin Sci (Lond). 2001; 101:159–68. [PubMed: 11473489]

47. De Yoreo JJ, Dove PM. Materials science. Shaping crystals with biomolecules. Science. 2004; 306:1301–2. [PubMed: 15550649]

48. Dombrose FA, Gitel SN, Zawalich K, Jackson CM. The association of prothrombin fragment 1 with phospholipid. Quantitative characterization of the Ca^{2+} ion-mediated binding of prothrombin fragment 1 to phospholipid vesicles and a molecular model for its association with phospholipids. J Biol Chem. 1979; 254:5027–40. [PubMed: 447632]

49. Gul A, Rez P. Models for binding to calcium oxalate surfaces. Urol Res. 2007; 35:63–71. [PubMed: 17372730]

50. Dawson CJ, Grover PK, Ryall RL. Inter-α-trypsin inhibitor in urine and calcium oxalate urinary crystals. Br J Urol. 1997; 81:20–6. [PubMed: 9467471]

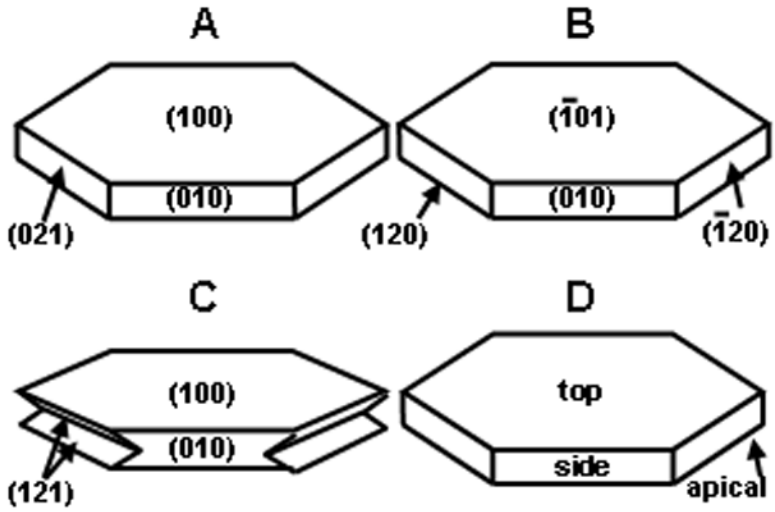

Fig. 1.

The common structure of uCOM (**A, B**) and iCOM (**C**) crystals, showing the Miller indices used by Wesson and colleagues (**A**) [18–20], Qiu and associates (**B**) [21–23], and the group of Hunter *et al*. (**C**) [24,25]. **D,** shows the system used in the present study, where the top, side and apical faces correspond, respectively, to the (100) (010) and (021) faces assigned by Tazzoli and Domeneghetti [26].

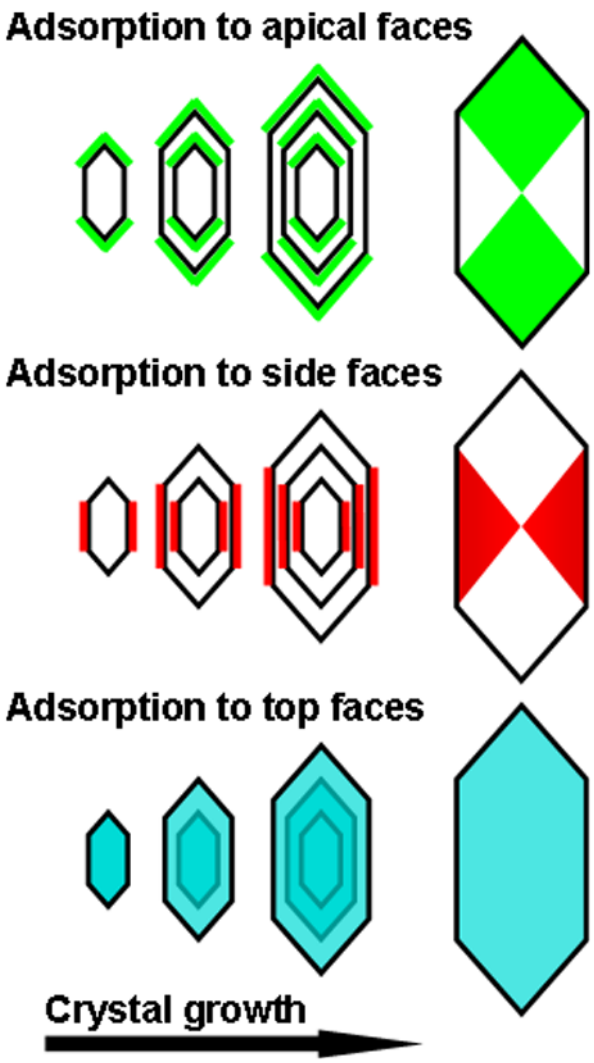

Fig. 2.
Expected intersectoral zoning of a fluorescently labelled protein after specific binding to each of the three dominant faces of COM, viewed from the top face of the crystal.

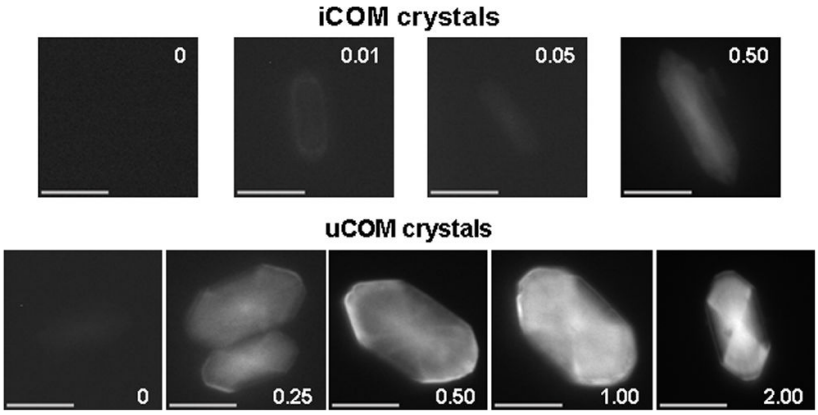

Fig. 3.

COM crystals grown from inorganic solutions (top row) and ultrafiltered human urine (bottom row) in the presence of PTF1 at the concentrations (mg/L) indicated. All crystals were photographed with an exposure time of 2.0s. Scale bar = 10 μm.

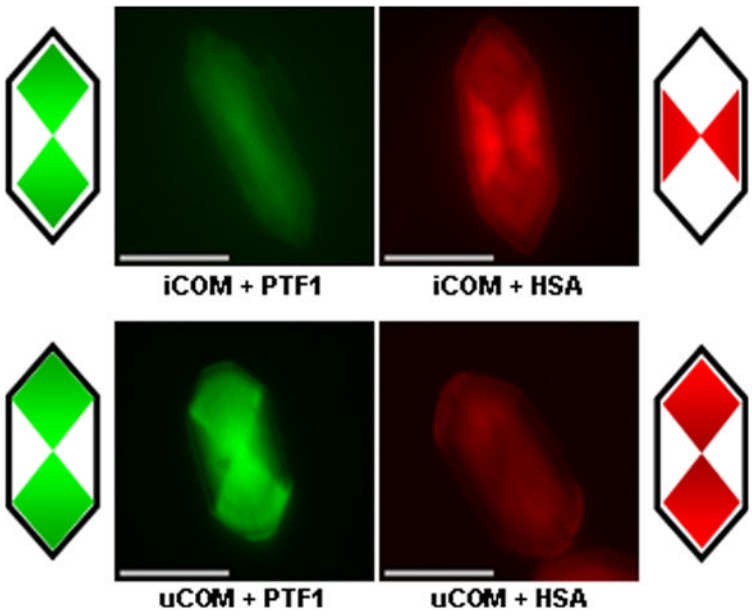

Fig. 4.

Intersectoral zoning of PTF1 (0.5 mg/L) and HSA (5 mg/L) in iCOM crystals (top row) and PTF1 (1 mg/L) and HSA (20 mg/L) in uCOM crystals (bottom row). Images were coloured using Adobe Photoshop 5.5 to facilitate comparison of fluorescent bow-tie patterns. PTF1 patterns are consistent with limited binding to the top COM face, but principally to the apical faces in both inorganic solutions and ultrafiltered urine. However, HSA binds predominantly to the side faces of COM under inorganic conditions, but to the apical faces in ultrafiltered urine. Cartoons depict the patterns of predominant fluorescence. Bars = 10 μm.

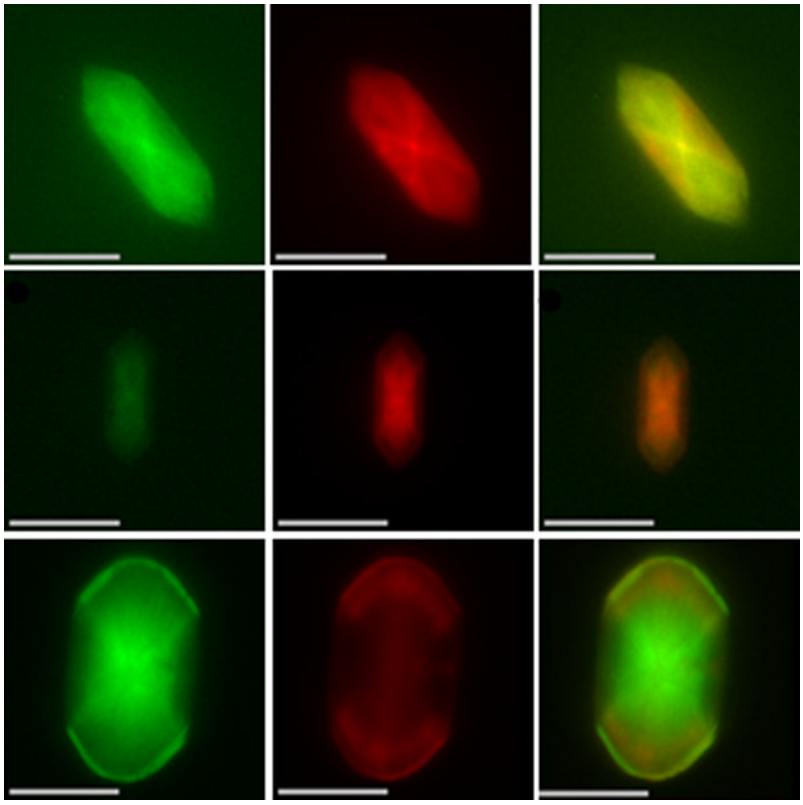

Fig. 5.

Typical intersectoral zoning patterns of PTF1 (green) and HSA (red) in iCOM crystal precipitated in the presence of both proteins, at the same final concentration of 0.05 mg/L (top row); iCOM crystal generated in an inorganic solution containing PTF1 and HSA at final concentrations of 0.04 mg/L and 2.0 mg/L, respectively (middle row); uCOM crystal deposited from ultrafiltered urine containing 2 mg/L PTF1 and 20 mg/L HSA (bottom row). Note that each row depicts the same crystal, photographed using different filters. PTF1 was labelled with FITC and HSA was tagged with Alexa Fluor-647. The right-hand column depicts overlays of the two patterns presented in the adjacent left-hand and middle columns. Bars = 10 μm.

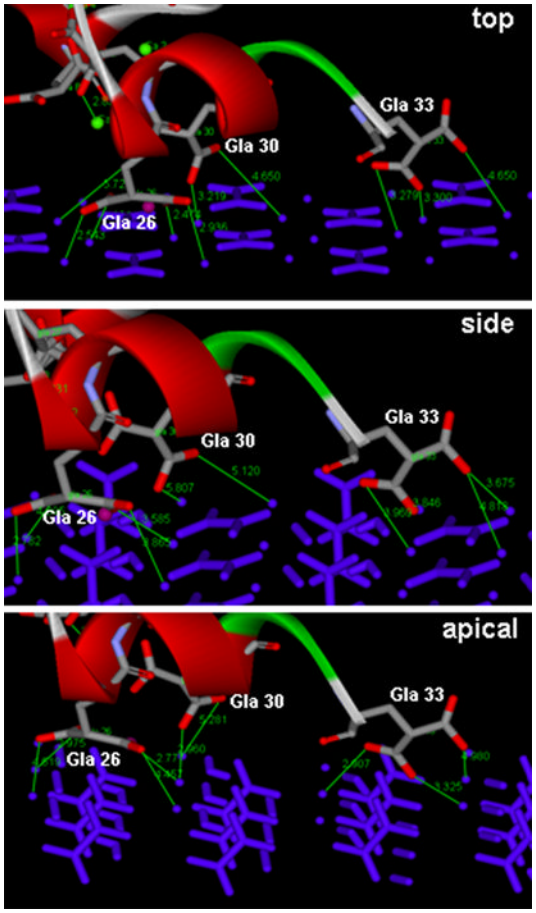

Fig. 6.

Interactions between oxygen atoms (red) of Gla residues 26, 30 and 33 of bovine PTF1 and calcium atoms (blue balls) on the top, side and apical surfaces of the COM crystal, modelled using Accelrys. Atomic distances in Ångströms are indicated by fine green lines.

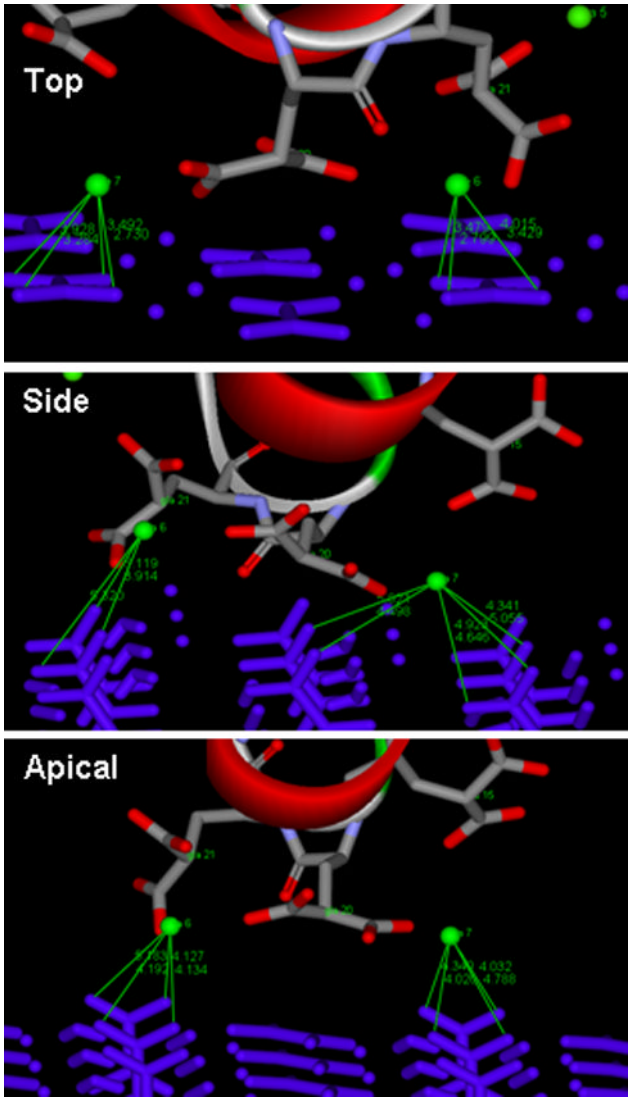

Fig. 7.
Interactions between Ca-6 and Ca-7 (green spheres) and oxygen atoms of oxalate groups (blue bars) on the top, side and apical surfaces of COM, simulated using Accelrys. Atomic distances in Ångstroms are indicated by fine green lines.

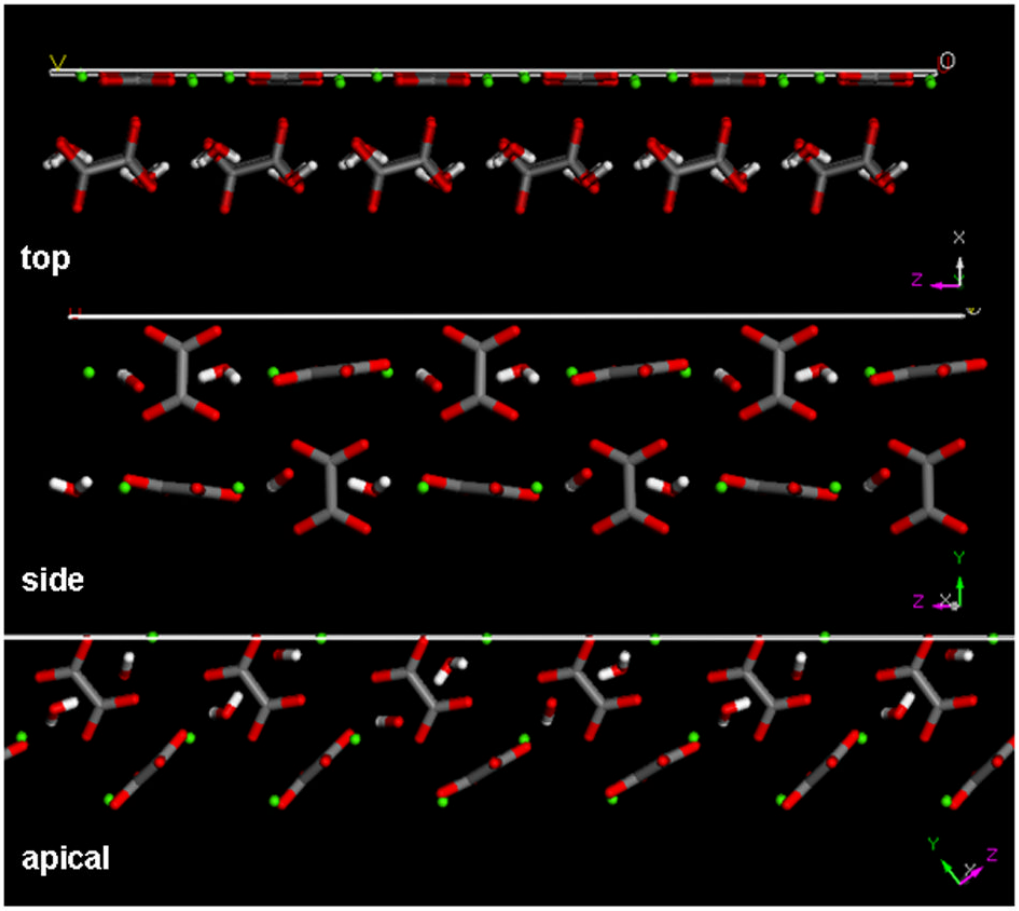

Fig. 8.
Side perspective view of the molecular structure of the top, side and apical faces of COM, simulated using Materials Studio (Accelrys). Green spheres depict calcium atoms, grey (carbon) and red (oxygen) structures are oxalate groups, white (hydrogen) and red (oxygen) stick figures are water molecules.

Table 1

Amino acid sequences of the Gla domains of human and bovine PTF1

	1								**10**								**20**								**30**								**40**	
Human[*]	A	N	T	F	L	γ	γ	V	R	K	G	N	L	γ	R	γ	C	V	γ	γ	T	C	S	Y	γ	γ	A	F	γ	A	L	γ	S	S	T	A	T	D	V	F	
Gla no.						6	7							14		16			19		20				25	26			29			32									
Bovine[†]	A	N	K	G	F	L	γ	γ	V	R	K	G	N	L	γ	R	γ	C	L	γ	γ	P	C	S	R	γ	γ	A	F	γ	A	L	γ	S	L	S	A	T	D	A	F
Gla no.							7	8							15		17			20	21					26	27			30			33								

[*]The human sequence was obtained from http://beta.uniprot.org/blast/?about = P00734[44–89 (Uniprot) and the

[†]bovine, from http://www.rcsb.org/pdb/explore/remediatedSequence.do?structureId = 2PF2 (Protein Data Bank). Gla residues are represented by γ symbols. Identical sequences are highlighted in yellow. Numbering is for the human sequence.